

CONTINUOUS- AND FIRST-ORDER PHASE TRANSITIONS IN ISING ANTIFERROMAGNETS WITH NEXT-NEAREST-NEIGHBOUR INTERACTIONS

A. Malakis, P. Kalozoumis and N. G. Fytas

Section of Solid State Physics, Department of Physics, University of Athens, Panepistimiopolis, GR 15784 Zografos, Athens, Greece

Received: December 08, 2006

Abstract. Both the square and triangular Ising antiferromagnetic systems with next-nearest neighbour interactions are studied by a new efficient entropic scheme. Using the energy distribution and order parameter's fourth order cumulant it is illustrated that the two models behave quite differently. For the square model we establish strong numerical evidence showing a continuous transition scaling, whereas for the triangular model a first-order transition is verified. Our results are compared with the existing predictions and controversies in the literature.

1. INTRODUCTION

Spin models with competing interactions are of great theoretical and experimental interest and have been for a long time the subject of many investigations. Such interactions give rise to complicated spatial orderings and produce complex and rich critical behavior [1,2]. The transitions between ordered and disordered phases may be continuous- or of first-order with a tricritical point between them, but no general classification exists, connecting the symmetry of spin structures and the range of interactions with the expected critical behavior. As is well known the Ising square lattice with nearest-neighbour (nn) coupling is an exactly solved model and almost all of its properties are known [3]. With the addition of next-nearest-neighbour (nnn) interactions the problem is no longer exactly soluble and several approximate methods have been applied to attack this more general problem

and to understand the effect of adding the nnn-coupling on the critical behavior of the system [4-11]. Of particular interest is the range of interactions, where the ground state is an arrangement with super-antiferromagnetic (SAF) order in which ferromagnetic rows (columns) alternate with opposite oriented spins. The system, in zero-field, is governed by the Hamiltonian:

$$H = J_{nn} \sum_{\langle i,j \rangle} S_i S_j + J_{nnn} \sum_{(i,j)} S_i S_j, \quad (1)$$

where here both nearest-neighbour (J_{nn}) and next nearest-neighbour (J_{nnn}) interactions are assumed to be positive (antiferromagnetic) and the system, as is well known [4-9,11], develops at low temperatures super-antiferromagnetic order for $R=J_{nnn}/J_{nn}>0.5$. Note that there is no loss of generality in considering only $J_{nn} > 0$ since the critical behavior associated with the SAF ordering is the same if

Corresponding author: A. Malakis, e-mail: amalakis@phys.uoa.gr

$J_{nn} \rightarrow -J_{nn}$. From now on we shall refer to this model, as the square SAF model.

Several previous studies have suggested that the above system may possess anomalous exponents, and a non-universal critical behavior with exponents depending on the coupling ratio R has been the commonly accepted scenario for many years [4-9,11]. However, recently the interest on the subject has been renewed and some attempts to re-examine the behavior of this model have taken place. In several papers Lopez *et al.* [12-14] have used the cluster variation method (CVM) to study this model and have concluded that the system undergoes a first-order transition for a particular range of the coupling ratio: $R = 0.5-1.2$. It appears that this scenario has been further supported by the study of Buzano and Pretti [15]. These authors studied the same model with an additional 4-body coupling, using again the CVM, and concluded that according to this method a first-order behavior is expected for a very large part of the parameter space reproducing also the results of Refs. [12-14]. However, they also considered the limiting case $J_{nn} = 0$, where the exact solution of Baxter model [16] applies, observing again a large part of the parameter space in which the CVM predicts first-order behavior. Thus, the CVM fails to predict the true second-order critical behavior for the Baxter model and, this is of course, an obvious reason for suspecting the CVM. It is quite possible that the CVM, in any finite order approximation, could produce misleading mean-field behavior not unlikely with other variational methods [17]. Notwithstanding that, a recent Monte Carlo simulation [18] of the analogous triangular model has suggested a first-order transition from the ordered to the paramagnetic phase. This last model includes also nn- and nnn-antiferromagnetic couplings but now the model is defined on the triangular lattice. Having to deal with the same Hamiltonian and a similar ground state arrangement (SAF arrangement) one should naively expect the same critical behavior for the two models, assuming a simple universality in which the underlying lattice is immaterial in 2D.

In the light of the above situation, it is of interest to follow again the traditional finite-size scaling analysis to re-examine the above predictions and controversies for both square SAF model and triangular SAF case. In the next Section we outline the entropic sampling technique implemented to generate numerical estimates for all thermal and magnetic properties in the critical region for the case $R = 1$. In Section 3 we explain why our numerical data are not supporting a first-order transi-

tion for the square SAF model. On the other hand, we present concrete evidence of a first-order transition for the triangular SAF model. Section 3 ends with a summary of finite-size scaling and the concept of weak universality for the square SAF model. Section 4 summarizes our conclusions.

2. THE CRMES WANG-LANDAU ENTROPIC SAMPLING SCHEME

Traditional Monte Carlo sampling methods have been used for many years in the study of critical phenomena [19-23] and the first Monte Carlo approaches to the present model were indeed carried out by the Metropolis algorithm [5-7]. On the other hand, general flat histogram methods [23-28] are alternatives to importance sampling and are expected to be much more efficient for studying a complex system. A simple and efficient entropic implementation of the Wang-Landau (WL) method has been presented recently by the present authors. This method is based on a systematic restriction of the energy space with increasing the lattice size. The random walk of this entropic simulation takes place only in the appropriately restricted energy space and this restriction produces an immense speed up of all popular algorithms calculating the density of energy states (DOS) of a statistical system [29,30]. For the temperature range of interest, which is the range around a critical point, this scheme determines all finite-size anomalies using an one-run entropic strategy employing what we have called the critical minimum energy subspace (CrMES) WL entropic sampling method. In this approach all (thermal and magnetic) properties are obtained from the high-levels of the WL random walk process by constructing appropriate microcanonical estimators. The method is efficiently combined with the N -fold way [31] in order to improve statistical reliability, but also to produce broad histogram (BH) estimators for an additional calculation of the DOS.

The approximation of canonical averages, in a temperature range of interest, is as follows:

$$\langle Q \rangle = \frac{\sum_E \langle Q \rangle_E G(E) e^{-\beta E}}{\sum_E G(E) e^{-\beta E}} \equiv \frac{\sum_{E \in (E_1, E_2)} \langle Q \rangle_{E, WL} \tilde{G}(E) e^{-\beta E}}{\sum_{E \in (E_1, E_2)} \tilde{G}(E) e^{-\beta E}}. \quad (2)$$

The restricted energy subspace (E_1, E_2) is carefully chosen to cover the temperature range of interest

without introducing observable errors. The microcanonical averages $\langle Q \rangle_E$ are determined from the $(E; Q)$ -histograms (denoted by $H_{WL}(E, Q)$), which are obtained during the high-levels of the WL process

$$\begin{aligned} \langle Q \rangle_E &\cong \langle Q \rangle_{E, WL} \equiv \sum_Q Q \frac{H_{WL}(E, Q)}{H_{WL}(E)}, \\ H_{WL}(E) &= \sum_Q H_{WL}(E, Q), \end{aligned} \quad (3)$$

and the summations run over all values generated in the restricted energy subspace (E_1, E_2) . Finally, the approximate DOS used in Eq. (2) is obtained from the DOS generated via the WL iteration ($\tilde{G}(E) = G_{WL}(E)$) or from the BH approximation ($\tilde{G}(E) = G_{BH}(E)$). As mentioned above, the updating of the appropriate histograms is carried out only in the high-levels of the WL process. In these stages, the incomplete detailed-balance condition has no significant effects on the microcanonical estimators constructed from the cumulative histograms, as shown in Ref. [30]. Thus we have used only the WL iterations: $j = 12-24$ for lattices up to $L = 100$ and the WL iterations: $j = 16-26$ for larger lattices. The initial modification factor of the WL process is taken to be $f_1 = e = 2.718\dots$ and, as usual, we follow the rule $f_{j+1} = \sqrt{f_j}$ and a 5% flatness criterion [29,30]. The performance limitations of entropic methods, such as the WL random walk and the reduction of their statistical fluctuations have recently attracted considerable interest [32-34]. For the CrMES entropic scheme applied here an extensive comparative study using various implementations was presented in Ref. [30].

In the present study, the accuracy of our data, for the square SAF model, was tested as follows: for a particular temperature, $T = 2.082$, close to the critical temperature, we have calculated, using long runs of the Metropolis algorithm, several thermodynamic properties of the system for $R = 1$. Let us briefly describe the method we obtained the Metropolis estimates (for instance the susceptibility values). First an initial equilibration period of $100 \times L^2$ usual Monte Carlo steps (lattice sweeps) was applied without updating the histograms. After thermalization, the updating of the histograms was applied in every Monte Carlo step, while the susceptibility values were determined and observed in time steps of $20 \times L^2$ Monte Carlo sweeps. A total of 300 such time steps (for all lattice sizes) were used, in the averaging, in order to obtain the equilibrium estimate for the susceptibility.

We have found good agreement with the corresponding estimates obtained via the entropic scheme described in the previous section. Fig. 1 illustrates this agreement by comparing, at this particular temperature, the magnetic susceptibility estimates (see below Eq. (9)) calculated by the Metropolis algorithm (χ_{Metr}) to those obtained from the entropic scheme (χ_{entr}). For the triangular SAF model, and for each lattice size ($L = 40-240$), we applied the above scheme to obtain accurate estimates for the DOS. Additionally, using these DOS estimates we performed a Lee-entropic scheme [34] to obtain our final estimates for all thermal and magnetic properties of the system.

In the present implementation of the CrMES method, we restrict the total energy range (E_{\min}, E_{\max}) to the minimum energy-subspace producing an accurate estimation for all finite-size anomalies. This restriction may be defined by requesting a specified accuracy on a diverging specific heat (or on a diverging susceptibility) as shown in [30]. Alternatively, the energy density function may be used in a simpler way to restrict the energy space. For a diverging specific heat (susceptibility) the pseudocritical temperature T_L^* is the temperature corresponding to the maximum of the specific heat (susceptibility). For the cumulant finite-size anomaly the pseudocritical temperature corresponds to the minimum of the cumulant. Thus, if \tilde{E} is the value maximizing the probability density, at some pseudocritical temperature (T_L^*), the end-points (\tilde{E}_{\pm}) of the energy critical subspaces (CrMES) may be located by the condition

$$\tilde{E}_{\pm} : \frac{P_{\tilde{E}_{\pm}}(T_L^*)}{P_{\tilde{E}}(T_L^*)} \leq r, \quad (4)$$

where r is chosen to be a small number, independent of the lattice size. Several values of r ($r = 10^{-3}$, $r = 10^{-4}$, $r = 10^{-5}$, and $r = 10^{-6}$) have been used in the present study to estimate the relevant extensions of critical subspaces discussed below. The resulting finite-size extensions of critical energy subspaces, denoted by $(\Delta \tilde{E})$, obey the specific heat's scaling law [29]

$$\Psi \equiv \frac{(\Delta \tilde{E})^2}{L^d} \approx L^{\frac{\alpha}{\nu}}. \quad (5)$$

Since the extensions of these energy subspaces satisfy very well the above scaling law, Eq. (5) is a new route for estimating the critical exponent α/ν [29,30]. Furthermore, following a similar procedure

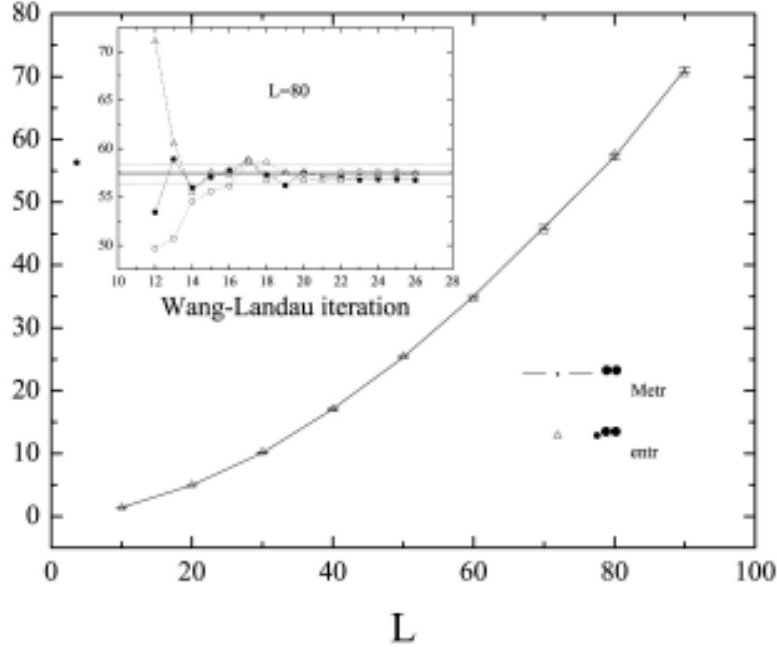


Fig. 1. Magnetic susceptibility estimates at $T = 2.082$ for both the Metropolis algorithm (χ_{Metr}) and the entropic WL scheme (χ_{entr}), for several lattices ($L = 10-90$). The solid line is a guide to the eye passing through the Metropolis estimates (shown with error bars), while triangles represent the estimates of the entropic scheme. The WL evolution of the estimates χ_{entr} for three random walks is illustrated in the inset for $L = 80$. Symbols in the inset show the entropic estimates converging to χ_{Metr} , illustrated for two Metropolis runs by the solid parallel lines. The range of the Metropolis fluctuations is indicated by the dotted parallel lines.

we may also estimate the critical exponent γ/ν , as already shown in [30]. Again, let \tilde{M} be the value maximizing the order-parameter density at some pseudocritical temperature, for instance at the susceptibility pseudocritical temperature ($T_L^* = T_L^*(\chi)$). The end-points (\tilde{M}_\pm) of the magnetic critical subspaces (CrMMS) are located by the condition

$$\tilde{M}_\pm: \frac{P_{\tilde{M}_\pm}(T_L^*)}{P_{\tilde{M}}(T_L^*)} \leq r, \quad (6)$$

and the corresponding finite-size extensions of critical magnetic subspaces obey close to a critical point, the susceptibility scaling law [30]:

$$\Xi \equiv \frac{(\Delta\tilde{M})^2}{L^d} \approx L^\gamma. \quad (7)$$

Eqs. (5) and (7) provide additional routes for estimating the involved critical exponents.

3. CONTINUOUS- VERSUS FIRST-ORDER PHASE TRANSITIONS. CRITICAL EXPONENTS - WEAK UNIVERSALITY OF THE SQUARE MODEL

Let us consider two different definitions for the order-parameter. First, with the help of four sublattices of the SAF ordering one may define a two-component order-parameter and finally use its root-mean-square (rms) as done in Ref. [6].

$$\begin{aligned} M_{\text{SAF}}^{(1)} &= \frac{M_1 + M_2 - (M_3 + M_4)}{4}, \\ M_{\text{SAF}}^{(2)} &= \frac{M_1 + M_4 - (M_2 + M_3)}{4}, \\ M_{\text{SAF}}^{(\text{rms})} &= \sqrt{(M_{\text{SAF}}^{(1)})^2 + (M_{\text{SAF}}^{(2)})^2}. \end{aligned} \quad (8)$$

An alternative and numerically more convenient definition will also be considered from the sum of

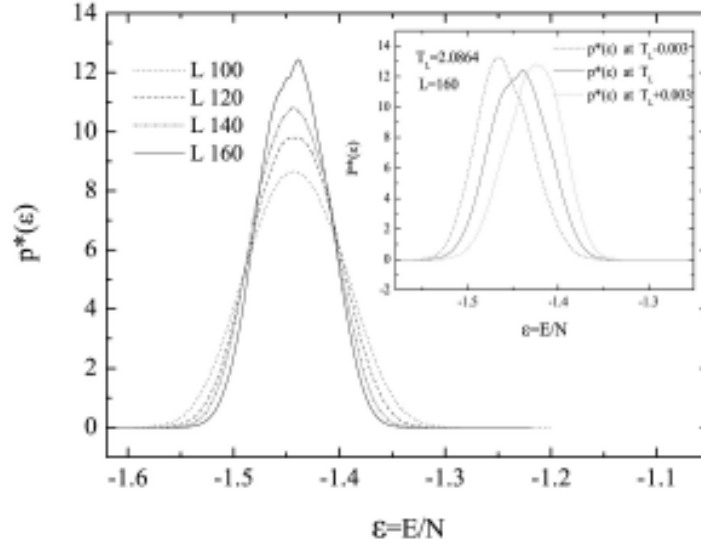


Fig. 2. Energy distributions for the square SAF model. The distribution for each lattice size has been computed at its respective specific heat's pseudocritical temperature. The inset shows the probability densities for the lattice $L = 160$ at the specific heat's pseudocritical temperature ($T_L^* = 2.0864$), as well as at two nearby temperatures ($T_L^* \pm 0.003$).

the absolute values of the four sublattice magnetizations

$$M_{SAF} = \sum_{i=1}^4 \frac{|M_i|}{4}. \quad (9)$$

The resulting behavior is very similar and in particular the finite-size extensions of the resulting CrMMS completely coincide supporting the equivalence of the two representations for the square SAF model. Therefore, for large lattices only the second order-parameter was used in order to minimize computer memory requirements.

Let us now consider the behavior of some properties of the system that may elucidate the nature of the phase transition from the low temperature ordered SAF phase to the high temperature paramagnetic phase. There are various kinds of criteria in the literature that attempt to characterize the order of a phase transition. Some of these are using theoretical arguments, such as the Landau-Lifshitz symmetry rules [18,35], but most attempts are based on the analysis of numerical data obtained from Monte Carlo studies of finite systems. A strong indication may be obtained by studying the form of finite-size scaling of the specific heat and susceptibility peaks and the scaling of the

pseudocritical (pseudo-transition) temperatures of the finite systems. From the theory of first-order transitions, developed by Binder and Landau [36] and Challa *et al.* [37], δ -like peaks scaling as L^d are expected for the specific heat and susceptibility peaks and the temperatures shifts are expected to vanish as L^{-d} ($T_L \cong T_c + bL^{-d}$). A finite-size analysis for the square SAF model with $R = 1$ will be presented in detail at the end of this section and as we shall see, a behavior characteristic of a second-order critical point, and not a first-order transition, will be observed. A supplementary characterization attempt, utilizing finite-size simulation data, is the illustration of the behavior of fourth order cumulants of energy and order-parameter distributions. Their behavior has been often used to emphasize the differences between the two types of transitions [36-42]. Finally, the existence of a pronounced double peak of the energy distribution at a pseudo-transition temperature has been considered as a strong signature of the coexistence of a low temperature phase with some energy E_- with a high temperature phase with some energy E_+ [18].

Fig. 2 presents the behavior of the energy distribution at the pseudocritical temperatures of the square SAF model for several lattice sizes. The inset illustrates the energy densities of a particular

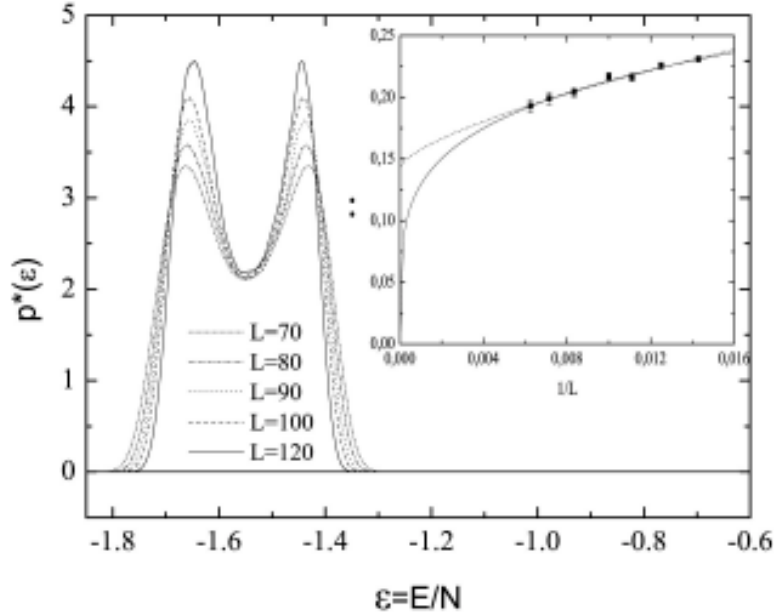


Fig. 3. Energy distributions for the triangular SAF model. The distribution for each lattice size has been computed at the temperature where the peaks are of equal height. The inset shows the variation of $\Delta\varepsilon = (E_+ - E_-)/N$ as a function of $1/L$.

case ($L = 160$) at temperatures in the neighbourhood of its pseudocritical temperature corresponding to the specific heat peak. Fig. 3 illustrates now the behavior of the energy distribution (at specific temperatures, see below) for the triangular model considered by Rastelli *et al.* [18]. The data used for the triangular model corresponds again to the interaction ratio $R = 1$ and were obtained by the same entropic scheme, described in previous Section, for several lattice sizes. The presence of the energy's double peak reported by Rastelli *et al.* [18] is very clear now. The temperatures, corresponding to each lattice shown in Fig. 3, were carefully chosen to yield two peaks of equal heights. These temperatures are very close, almost identical, to the pseudocritical temperature corresponding to the maximum of the specific heat of the finite systems.

Comparing the behavior of the energy distribution of the two models we may emphasize the strong difference in their behavior. Although in the case of the triangular lattice the existence of the double peaks may be thought as a finite-size signature of a first-order transition, as supposed by the authors of Ref. [18], the behavior for the square SAF model does not show similar signs, but rather

is characteristic of a second-order critical point. There are some points that should be noted about the above figures before moving to the illustration of the fourth order cumulants of the two models. In the case of the square SAF model there are some finite-size effects appearing in the structure of the energy density. These can be observed, close to the pseudocritical temperatures for large lattices, in the neighbourhood of the density peak as shown in Fig. 2 for the case $L = 160$. These are weak effects, observable for large enough lattices, and seem to persist for even larger lattices, as we have verified by simulating systems of sizes up to $L = 240$. However, a double peak structure is not emerging even at these sizes. On the other hand, the clear double peak structure for the triangular SAF model yields the inset of Fig. 3, describing the variation (with $1/L$) of the difference in energy of the two peaks defined by: $\Delta\varepsilon = (E_+ - E_-)/N$. A fit of our data to a power law with three free parameters ($\Delta\varepsilon = \varepsilon_0 + bL^{-w}$) yields the dashed line shown in the inset corresponding to a latent heat $\varepsilon_0 = 0.14(4)$, and this is to be compared with the value $\varepsilon_0 = 0.176(6)$ given in Ref. [18]. Nevertheless, the above fit has the same χ^2 per degree of freedom with a two-parameter power law of the form $\Delta\varepsilon = bL^{-w}$, il-

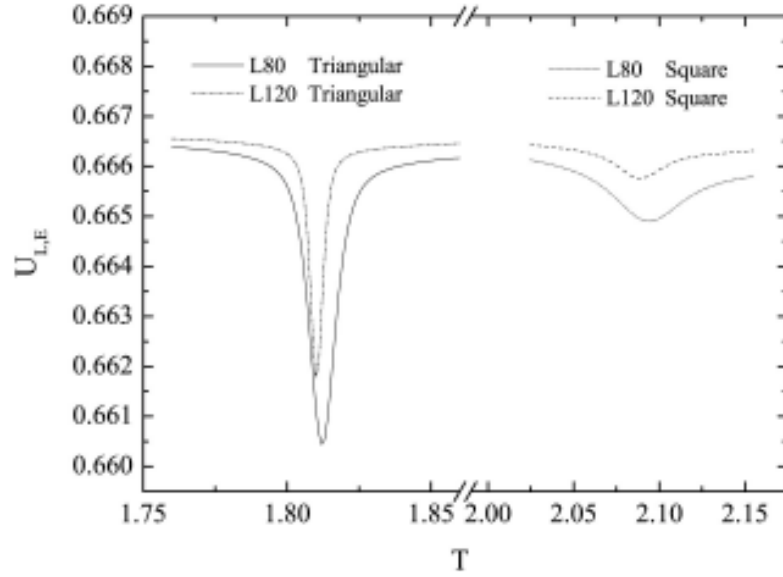


Fig. 4. Energy's reduced fourth order cumulants for the triangular and the square SAF model.

illustrated in the inset by the solid line. This last fit gives a value for the exponent w which is consistent with the scaling of the specific heat peaks, which however, does not conclusively support a scaling of the form L^d , as expected for a first-order transition. This may be a crucial discrepancy and was also observed in Ref. [18]. One can not completely exclude, at least at these lattice sizes, the possibility that the observed double peak is a strong finite-size effect that may cease to exist at the thermodynamic limit. However, our simulations for even larger lattice sizes, up to $L = 480$, support the proposal of Rastelli *et al.* [18] for a first-order transition.

We now turn to the finite-size behavior of the fourth order cumulants of the energy and the order-parameter, discussing again the differences between the square SAF model considered by Lopez *et al.* [12-14] and the triangular SAF model considered by Rastelli *et al.* [18]. Consider first the reduced energy cumulant, known also as Binder's reduced fourth order cumulant, defined by:

$$U_{L,E} = 1 - \frac{\langle E^4 \rangle}{3 \langle E^2 \rangle^2}. \quad (10)$$

Fig. 4 presents, in the same illustration, the behavior of both models. As one can see from this figure

the behavior of the square model is again characteristic of a second-order critical point. The very deep minimum for the triangular model, found also in Ref. [18], is a reflection of the very sharp specific heat peak and according to [18] is indicating a first-order transition. The differences in the behavior between the two models appear even stronger if we consider the connected form of the energy cumulant [38] (not shown) where a deep oscillation occurs close to the minimum for the triangular model.

Finally, consider the reduced fourth order cumulant of the order parameter defined, with the help of Eq. (9), as follows:

$$V_{L,M} = 1 - \frac{\langle M^4 \rangle}{3 \langle M^2 \rangle^2}. \quad (11)$$

As previously, Fig. 5 presents the behavior of both models. The very deep minimum appearing for the triangular model is now contrasted with the behavior of the square SAF model, which again reminds the characteristic behavior of a second-order critical point. The differences in behavior are similar if we use the rms order-parameter definition given in Eq. (8) instead of Eq. (9). They are even stronger if we use the connected form of cumulants [38], where oscillatory structures occur. Thus, our find-

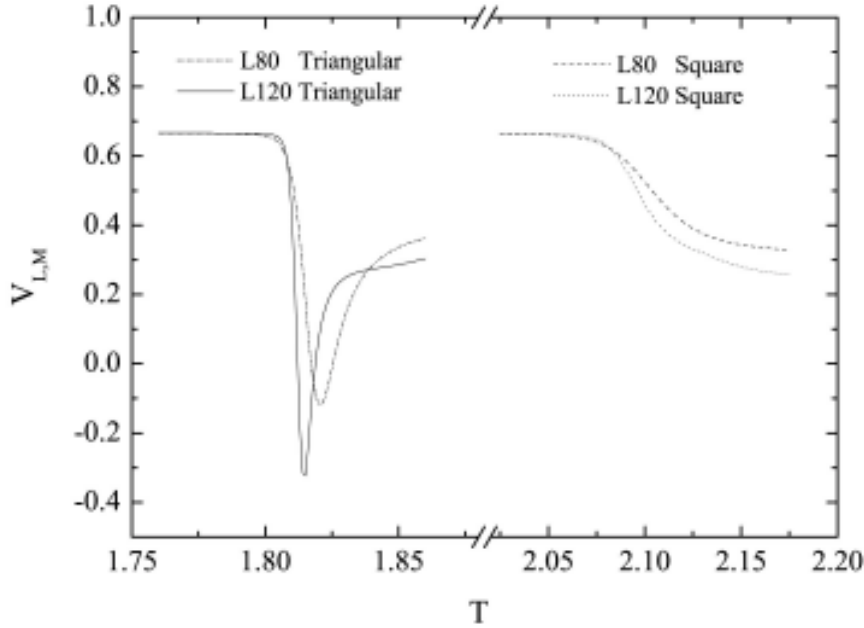


Fig. 5. Order-parameter's reduced fourth order cumulants for the triangular and the square SAF model.

ings for the triangular model are in good agreement with the properties reported in Ref. [18], while for the square SAF model a behavior characteristic of a second-order critical point seems to govern the finite systems for all properties studied. It appears that the first-order prediction of the CVM is incorrect, at least for the case $R = 1$.

Finally, let us present in more detail the finite-size behavior of the square SAF model. By using the crossing method [39] for the order-parameter cumulant we have previously [43] estimated the critical temperature for the case $R = 1$ (square SAF model) to be $T_c = 2.0823(17)$, and the shift exponent was estimated from various pseudocritical

temperatures to be of the order of $\lambda = 1.20(4)$. Furthermore, we have shown in Ref. [43] that the critical exponents for the square SAF model obey very well the hypothesis of weak universality, according to which the reduced critical exponents, i.e. $\hat{\gamma} = \gamma/\nu$; $\hat{\beta} = \beta/\nu$; $\hat{\phi} = (2-\alpha)/\nu$, are constant independent of the value of R and therefore have the 2D Ising values ($R \rightarrow \infty$), i.e. $\gamma/\nu = 1.75$, $\beta/\nu = 0.125$, and $(2-\alpha)/\nu = 2$ [6,44]. Additionally, let us present in Table 1 estimates for the exponents γ/ν and α/ν for several values of the accuracy factor r , obtained via the CrMES method (see Eqs. (4) and (6) and Refs. [29, 30]). All the values estimated also in our previous paper [43] are consistent with the weak uni-

Table 1. Estimates for the exponents γ/ν and α/ν for different values of r (accuracy of CrMES). For more details and definitions see Ref. [43].

r	$\Xi(T_L^*(\chi))$ γ/ν	$\Xi(T_c)$ γ/ν	$(\Psi(T_L^*) + \Psi(T_c))/2$ $\alpha/\nu (L = 10-160)$	$(\Psi(T_L^*) + \Psi(T_c))/2$ $\alpha/\nu (L = 50-160)$
10^{-3}	1.7680(11)	1.7433(82)	0.407(3)	0.424(6)
10^{-4}	1.7604(49)	1.7595(23)	0.412(2)	0.412(4)
10^{-5}	1.7604(57)	1.7590(38)	0.421(1)	0.424(4)
10^{-6}	1.7536(45)	1.7545(27)	0.426(3)	0.416(2)

versality conjecture, and in particular the exponents α and ν are estimated with great accuracy to be $\alpha/\nu = 0.412 \pm 0.005$ and $\nu = 0.8292 \pm 0.0024$.

4. CONCLUSIONS

The above numerical evidence give a very strong verification that the transition of the square SAF model is continuous, contrary to the prediction of the cluster variation method [12-14]. On the other hand, for the triangular SAF model we have further verified the existence of the first-order transition as first reported by Rastelli *et al.* [18], by showing that the finite-size behavior of the system is in close agreement in its main points with the behavior predicted by the first-order theory developed by Lee and Kosterlitz [45]. Details of this extensive verification will be published in a separate paper.

In conclusion, in this paper we have shown that the prediction of the cluster variation method of a first-order transition for the square SAF model is incorrect and the original scenario [4-9,11] of a non-universal critical behavior with exponents depending on the coupling ratio has been strongly reinforced and weak universality [6,44] is well obeyed. Finally, for the triangular SAF model we have presented decisive evidence that its phase transition is of first-order, in agreement with Ref. [18].

ACKNOWLEDGEMENTS

This research was supported by the Special Account for Research Grants of the University of Athens (ELKE) under Grant Nos. 70/4/4071. N. G. Fytas would like to thank the Alexander S. Onassis Public Benefit Foundation for financial support.

REFERENCES

- [1] W. Selke, In: *Phase Transitions and Critical Phenomena*, ed. C. Domb and J.C. Lebowitz (Academic Press London, 1992) vol.15. p1.
- [2] M. J. Velgakis and J. Oitmaa // *J. Phys. A* **21** (1988) 547.
- [3] L. Onsager // *Phys. Rev.* **65** (1944) 117; R. J. Baxter, *Exactly Solved Models in Statistical Mechanics* (Academic Press, London, 1982); B. McCoy and T. Wu, *The Two Dimensional Ising Model* (Harvard University Press, Cambridge, 1972).
- [4] M. P. Nightingale // *Phys. Lett. A* **59** (1977) 468.
- [5] R. H. Swedensen and S. Krinsky // *Phys. Rev. Lett.* **43** (1979) 177.
- [6] K. Binder and D. P. Landau // *Phys. Rev. B* **21** (1980) 1941.
- [7] D. P. Landau // *Phys. Rev. B* **21** (1980) 1285.
- [8] J. Oitmaa // *J. Phys. A* **14** (1981) 1159.
- [9] D. P. Landau and K. Binder // *Phys. Rev. B* **31** (1985) 5946.
- [10] J. Oitmaa and M. J. Velgakis // *J. Phys. A* **20** (1987) 1269.
- [11] K. Minami and M. Suzuki // *J. Phys. A* **27** (1994) 7301.
- [12] J. L. Moran-Lopez, F. Aguilera-Granja and J. M. Sanchez // *Phys. Rev. B* **48** (1993) 3519.
- [13] J. L. Moran-Lopez, F. Aguilera-Granja and J. M. Sanchez // *J. Phys. C* **6** (1994) 9759.
- [14] E. Lopez-Sandoval, J. L. Moran-Lopez and F. Aguilera-Granja // *Solid State Commun.* **112** (1999) 437.
- [15] C. Buzano and M. Pretti // *Phys. Rev. B* **56** (1997) 636.
- [16] R. J. Baxter // *Ann. Phys. (N.Y.)* **70** (1972) 193.
- [17] A. Malakis // *J. Phys. A* **14** (1981) 2767; *J. Stat. Phys.* **27** (1982) 1.
- [18] E. Rastelli, S. Regina and A. Tassi // *Phys. Rev. B* **71** (2005) 174406.
- [19] N. Metropolis, A. W. Rosenbluth, M. N. Rosenbluth, A. H. Teller and E. Teller // *J. Chem. Phys.* **21** (1953) 1087.
- [20] A. B. Bortz, M. H. Kalos and J. L. Lebowitz // *J. Comput. Phys.* **17** (1975) 10.
- [21] K. Binder // *Rep. Prog. Phys.* **60** (1977) 487.
- [22] M. E. J. Newman and G. T. Barkema, *Monte Carlo Methods in Statistical Physics* (Clarendon Press, Oxford, 1999).
- [23] D. P. Landau and K. Binder, *A Guide to Monte Carlo Simulations in Statistical Physics* (Cambridge University Press, 2000).
- [24] J. Lee // *Phys. Rev. Lett.* **71** (1993) 211.
- [25] B. A. Berg and T. Neuhaus // *Phys. Rev. Lett.* **68** (1992) 9.
- [26] J. -S. Wang and R. H. Swendsen // *J. Stat. Phys.* **106** (2002) 245; J. -S. Wang, T. K. Tay and R. H. Swendsen // *Phys. Rev. Lett.* **82** (1999) 476.
- [27] F. Wang and D. P. Landau // *Phys. Rev. Lett.* **86** (2001) 2050; *Phys. Rev. E* **64** (2001) 056101.
- [28] P. M. C. de Oliveira, T. J. P. Penna and H. J. Herrmann // *Braz. J. Phys.* **26** (1996) 677.
- [29] A. Malakis, A. S. Peratzakis and N. G. Fytas // *Phys. Rev. E* **70** (2004) 066128.

- [30] A. Malakis, S. S. Martinos, I. A. Hadjiagapiou, N. G. Fytas and P. Kalozoumis // *Phys. Rev. E* **72** (2005) 066120.
- [31] B. J. Schulz, K. Binder and M. Muller // *Int. J. Mod. Phys. C* **13** (2001) 477.
- [32] P. Dayal, S. Trebst, S. Wessel, D. Würtz, M. Troyer, S. Sabhapandit and S. N. Coppersmith // *Phys. Rev. Lett.* **92** (2004) 097201.
- [33] C. Zhou and R. N. Bhatt // *Phys. Rev. E* **72** (2005) 025701(R).
- [34] H.K. Lee, Y. Okabe and D.P. Landau // *Comput. Phys. Commun.* **175** (2006) 36.
- [35] E. Domany, M. Schick, J. S. Walker and R. B. Griffiths // *Phys. Rev. B* **18** (1978) 2209.
- [36] K. Binder and D. P. Landau // *Phys. Rev. B* **30** (1984) 1477.
- [37] M. S. S. Challa, D. P. Landau and K. Binder // *Phys. Rev. B* **34** (1986) 1841.
- [38] S.-H. Tsai and S.R. Salinas // *Braz. J. Phys.* **28** (1998) 58.
- [39] K. Binder // *Phys. Rev. Lett.* **47** (1981) 693; *Z. Phys. B* **43** (1981) 119.
- [40] A. Billoire, R. Lascaze, A. Morel, S. Gupta, A. Irback and B. Peterson // *Phys. Rev. B* **42** (1990) 6743.
- [41] K. Vollmayr, J. D. Reger, M. Scheucher and K. Binder // *Z. Phys. B* **91** (1993) 113.
- [42] K. Binder and D. W. Heermann, *Monte Carlo Simulations in Statistical Physics* (Springer-Verlag, Berlin, 1998).
- [43] A. Malakis, P. Kalozoumis and N. Tyraskis // *Eur. Phys. J. B* **50** (2006) 63.
- [44] M. Suzuki // *Prog. Theor. Phys.* **51** (1974) 1992.
- [45] J. Lee and J. M. Kosterlitz // *Phys. Rev. B* **43** (1991) 3265.